JOURNAL OF CATALYSIS 127, 366–376 (1991)

Structural Studies of Platinum/ZSM-5 Catalysts

EFIM S. SHPIRO,* RICHARD W. JOYNER,†,[1] KHABIB M. MINACHEV,* AND PAUL D. A. PUDNEY†

*N. D. Zelinksy Institute of Organic Chemistry, USSR Academy of Sciences, Moscow, USSR; and †Leverhulme Centre for Innovative Catalysis and Surface Science Research Centre, University of Liverpool, PO Box 147, Grove Street, Liverpool L69 3BX, United Kingdom

Received December 15, 1989; revised July 3, 1990

Pt/ZSM-5 catalysts have been prepared, characterised by extended X-ray absorption fine structure (EXAFS), and electron microscopy, and their activity in ethane hydrogenolysis has been measured. Calcination temperature is important in determining the size of the platinum particles formed. For a 0.5% Pt/H–ZSM-5 catalyst calcined at 720 K and reduced at 620 K or 790 K, small particles within the zeolite framework are observed, with a nearest neighbour coordination number of ca. 6 and an average diameter of about 8 Å. Calcination of a similar catalyst at 790 K resulted in larger metal particles, with the average diameter in the range 12–15 Å, estimates from EXAFS and electron microscopy being in agreement within experimental error. Contractions of up to 4% in the average Pt–Pt interatomic distance were observed, but there is clear evidence that the larger particles at least retain the face-centred cubic structure. EXAFS indicates the presence of Pt–O bonding as a result of coordination to the zeolite framework, with bond lengths of 1.92–2.03 Å. These catalysts have higher specific activity in ethane hydrogenolysis and alkane aromatization than materials where the platinum is in the form of large particles, ($d > 100$ Å), at the external surface of the zeolite, and reasons for this are discussed.

INTRODUCTION

There continues to be considerable interest in the properties of catalysts in which noble metals are combined with zeolites. The intrinsic catalytic activity of platinum or other metals may be enhanced and there is also the possibility of synergy between the metal and the zeolite. In this paper we discuss mainly structural aspects of small platinum clusters in H–ZSM-5 zeolite catalysts. These materials exhibit interesting catalytic properties in C_2 and C_3 alkane aromatization (*1*), and it has been suggested, based on XPS evidence, that the metal particles are electron deficient (*2*). The technique of choice is X-ray absorption spectroscopy, and in particular extended X-ray absorption fine structure (EXAFS). The structure of platinum particles has been studied in faujasitic zeolites, e.g., by Moraweck and Renouprez (*3*) using EXAFS, and by Gallezot *et al.* (*4*), using EXAFS and radial distribution function measurements. The only previous structural study of the zeolite ZSM-5 relates to the location of Ni^{2+} ions exchanged into the framework (*5*).

The EXAFS technique has been applied to the study of catalysts for about 10 years (*6*), but can still arouse scepticism about its quantitative accuracy (witness some of the discussion at the 1988 International Congress on Catalysis (*7*)). A number of approaches have been used to extract interatomic distances and coordination numbers from the spectra, and experimental error has been either ignored completely or estimated subjectively. Recently Joyner *et al.* (*8*) published a statistical test which allows a quantitative estimate of the error bar on any individual result and considers correlation between parameters; here this approach is applied rigorously.

[1] To whom correspondence should be addressed.

0021-9517/91 $3.00

EXPERIMENTAL

1. Materials

Techniques of zeolite and catalyst preparation have been described previously (*1*). Samples (10 g) of NH_4–ZSM-5, SiO_2/Al_2O_3 ratio 33/1, were exchanged with and subsequently impregnated from aqueous solutions of platinum (II) tetrammine dichloride. Three catalysts were investigated, two samples with 0.5 wt% Pt, calcined respectively at 720 and 790 K, and a 1% Pt sample calcined at 790 K. Calcination was performed in flowing dry air, with a two-stage temperature ramp; the temperature was raised to 620 K at a rate of 1.3 K min^{-1}, held at this temperature for 30 min, raised to the upper temperature at 3 K per min, and held there for 3 h.

2. Procedure

EXAFS measurements were performed at the SERC Daresbury synchrotron radiation source, using a dipole magnet source (Station 7.1) and an *in situ* cell which has been described before (*9*). Samples were in the form of pressed 13-mm-diameter disks, with a typical thickness of 1 mm. Samples were treated in flowing gases at 1 bar and 60 ml min^{-1} flow rate, and cylinder gases (from BOC plc) were used without further purification. Spectra of the Pt L_{III} edge were measured with the radiation source operating at 2 GeV energy and beam currents of 150–250 mA: spectral acquisition time was typically 1 h and three spectra were usually averaged. Spectra were collected up to 400 eV above the absorption edge ($\mathbf{k} = 10$ Å^{-1}). The spectrum of a platinum foil was acquired simultaneously and used to look for changes in the position of the X-ray absorption edge of the catalyst samples.

The procedure for catalytic measurements has been described elsewhere (*10*).

3. Data Analysis Techniques

Spectra were processed and analysed using standard techniques developed at the SERC Daresbury Laboratory. Background subtraction used the programme EXBACK and theory/experiment comparisons were performed with the programme EXCURV88, which makes an interactive point-by-point calculation of the EXAFS, using predetermined phase shifts and treating the photoelectron as a curved wave (*11, 12*). The programme minimises the least-squares fitting index between theory and experiment, FI, which is defined and discussed elsewhere (*8*). Important additional features of the EXCURV88 programme are the ability to plot a contour map showing the way in which FI varies with any two parameters, and also to calculate the correlation matrix for all of the parameters used in any fit.

Phase shifts were obtained from the Daresbury EXAFS data base (*13*), and were refined in the programme EXCURV88, by comparison to the spectrum of a platinum foil. Refinements to the central atom and Pt backscattering atom phase shifts were carried out over the same range (3–10 Å^{-1}, 40–400 eV above the absorption edge), in which the catalyst spectra were analysed. We estimate that any systematic errors introduced into the fit by the phase shifts do not exceed 0.005 Å for the Pt–Pt nearest neighbour distance.

The contribution of any shell of neighbours to a fit has been assessed by the significance test described previously (*8*). A shell is accepted only if there is $<5\%$ probability that the improvement in fit from the inclusion of that shell could be the result of random noise; for most of the shells reported here the probability is $<1\%$. The estimation of the error of any individual result is achieved by application of a similar criterion, by examination of the correlation matrix and use of the contour map. We therefore include the correlation of the most important parameters in the assessment of error; interatomic distances are normally strongly correlated only with the energy zero of the photoelectron (which EXCURV88 treats as a disposable parameter), while coordination numbers usually

TABLE 1

EXAFS Results for a 0.5% Pt/ZSM-5 Catalyst Precalcined at 720 K

	Pt–O		Pt–Pt	
	N	*R* (Å)	*N*	*R* (Å)
Reduced at 620 K[a]	1.0 ± 0.3	1.91 ± 0.03	4.6 ± 1.3	2.66 ± 0.01
Reduced at 790 K[a]	0.8 ± 0.3	1.93 ± 0.03	5.9 ± 1.3	2.68 ± 0.01
Reduced at 790 K, then exposed to O_2 at 298 K	2.1 ± 0.3 4.6 ± 0.6	1.96 ± 0.03 2.23 ± 0.03	2.9 ± 0.7	2.63 ± 0.01

[a] Spectra were measured *in vacuo* (ca 1×10^{-6} Torr) after reduction in flowing hydrogen at 1 bar pressure.

correlate highly with the relevant Debye–Waller factors.

This approach to data analysis avoids the use of Fourier transform or filtering procedures. Although these are useful in some cases and improve the appearance of experimental data by eliminating high-frequency noise, they introduce statistical correlation between data points. As a result, quantitative assessment of experimental error becomes very difficult.

RESULTS

Two catalysts containing 0.5% platinum by weight were studied to determine the influence of calcination temperature on the resultant platinum particle size. The results for the catalyst calcined at 720 K are given in Table 1; the catalyst has been examined after reduction at 620 K, after a further reduction at 790 K, and following exposure to oxygen at 298 K. Figure 1a shows a typical example of the quality of fit obtained between experimental and calculated EXAFS and the inclusion of a platinum–oxygen distance as well as a Pt–Pt distance should be noted. Figure 1b shows the theory–experiment comparison obtained when the platinum–oxygen distance is excluded from the fit and it can be seen that agreement is significantly worse, particularly below 8 $Å^{-1}$.

More detailed experiments, including examination of the as-received material, have been carried out for a 0.5% Pt catalyst calcined at 790 K, and also for a 1% Pt catalyst calcined at 790 K. The 1% sample was also investigated after reduction and exposure to oxygen at 298 K. The results of the data analysis are given in Tables 2 and 3. In accordance with XPS studies (*2*), calcination can be sufficient to reduce some platinum to the metallic state. Also, the average size of the Pt particles, as indicated by the nearest neighbour coordination number (CN), increases significantly as a result both of higher calcination temperature and of increased metal loading. One consequence of this is that it is necessary to include nonnearest neighbour Pt–Pt distances to achieve a good description of the experimental data. Figure 2 shows a fit to the 1% loading data using five shells of neighbours, again including a Pt–O shell. Statistical analysis shows that inclusion of each of these shells generates a significant improvement in the fitting index.

The 0.5% Pt sample calcined at 790 K was examined after reduction at 620 K, both in hydrogen at 1 bar and in vacuum (1×10^{-6} Torr), and after a further reduction at 790 K, again both in hydrogen and in vacuum. As indicated in Table 2, the calculated particle parameters were found to be the same

TABLE 2

EXAFS Results for a 0.5% Pt/ZSM-5 Catalyst Precalcined at 790 K

		N	*R* (Å)
As received	Pt–O	8.5 ± 2	2.16 ± 0.02
	Pt–Pt	2.4 ± 0.3	3.72 ± 0.02
Reduced[a]	Pt–O	2.5 ± 1	1.94 ± 0.02
	Pt–Pt	9.3 ± 1	2.75 ± 0.01
		3.9 ± 0.6	3.89 ± 0.03
		8.0 ± 1	4.79 ± 0.02
		3[b]	5.38[b]

[a] The same results, within experimental error, were observed after reduction at 620 and 790 K and a measurement in hydrogen (1 bar) or vacuum (1×10^{-6} Torr).

[b] Values for this shell are complicated by multiple scattering; errors are thus difficult to assess.

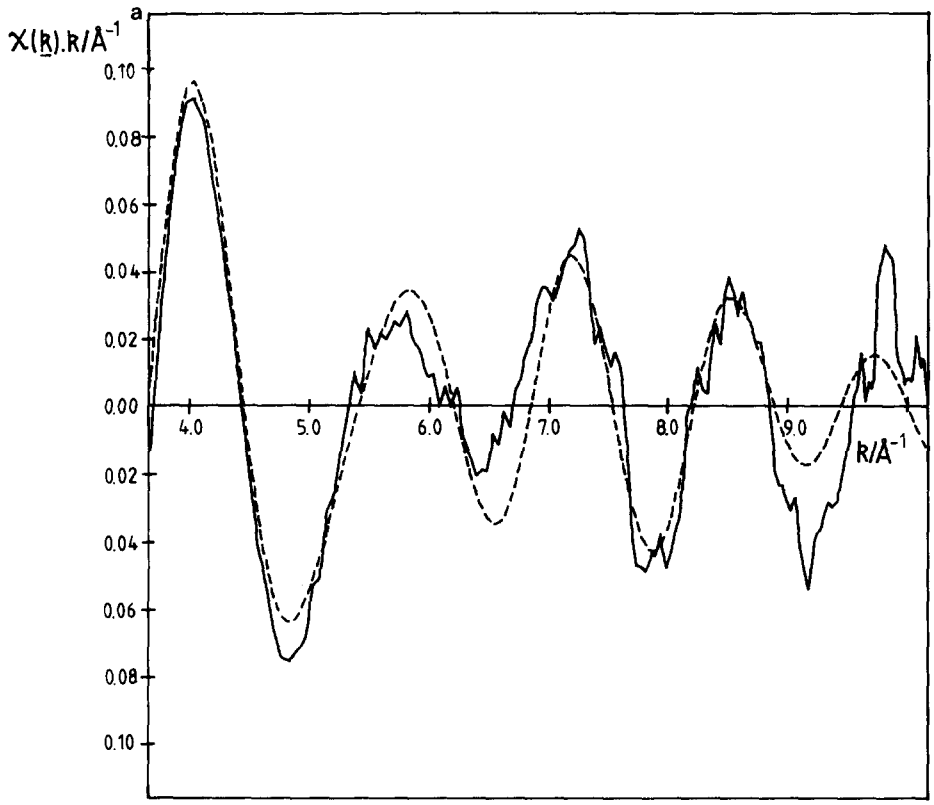

FIG. 1a. Experimental (solid line) and calculated (dashed line) EXAFS for a 0.5% Pt/HZSM-5 catalyst which has been calcined at 720 K and reduced at 790 K. Parameters used in the calculation are given in Table 1.

within experimental error. No shifts in the position of the platinum L_{III} edge were noted in any of these studies.

The catalytic activity of two of these materials in the hydrogenolysis of ethane has been measured, and the results are reported in Table 4. This table also indicates the turnover numbers and other data for two Pt/H–ZSM catalysts which have been prepared and reduced without a calcination step. Examination of these materials by electron microscopy and CO chemisorption indicated that the majority of the platinum was present in the form of large particles, d > 100 Å, at the external surface of the zeolite. These catalysts were not examined by EXAFS, since the technique is not sensitive at large particle size.

DISCUSSION

The main aspects of the structural results which we discuss are the particle size and shape, the observation of platinum–oxygen distances in all three cases, and the change in Pt–Pt nearest neighbour distance with respect to that in bulk platinum. We also relate these results to the catalytic properties of these materials.

1. Particle Structure, Size, and Shape

Both absolute and relative coordination numbers provide information about the average size and shape of the metal particles, as pointed out by Joyner (*14*) and Greegor and Lytle (*15*). The nearest neighbour metal–metal coordination number is the most accurate, and provides the best indica-

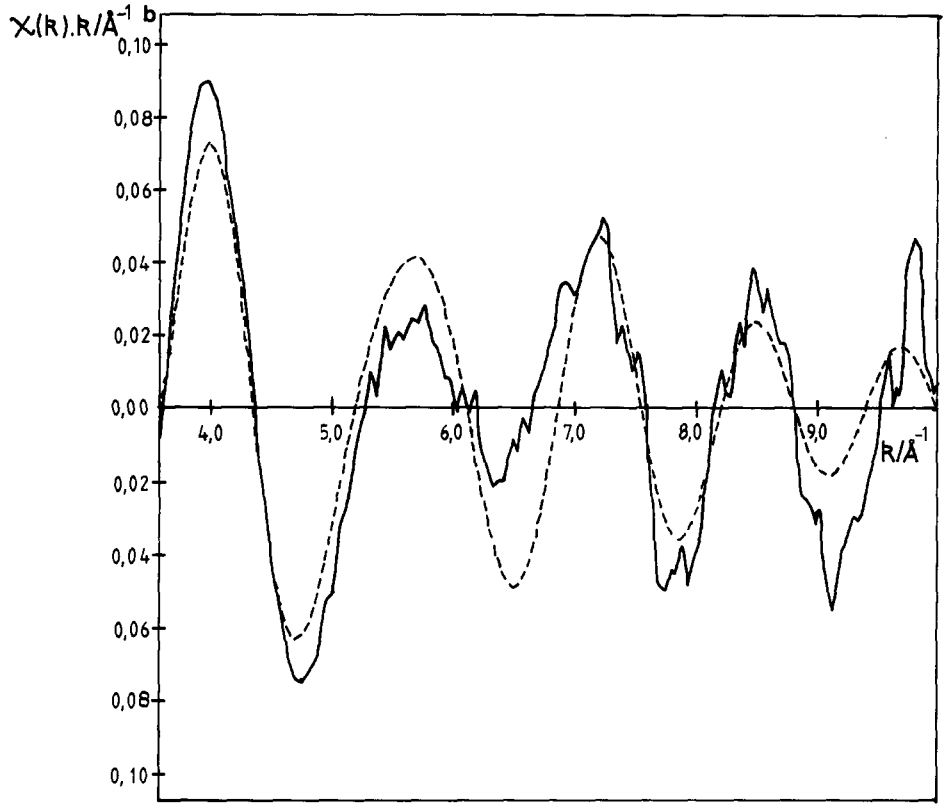

FIG. 1b. As in 1a, but excluding platinum–oxygen bonding from the calculation.

tor of particle size. We have estimated the average number of atoms in our particles from a consideration of the nearest neighbour coordination number calculated for face-centred cubic clusters containing "magic numbers" of atoms, e.g., 13, 33, 43, 55, 116, 147, and 309. It should be noted that this approach gives significantly larger estimates of the number of atoms per particle than can be deduced from the figures in the paper of Greegor and Lytle (*15*). From the average number of atoms in the particle

TABLE 3

EXAFS Results for a 1% Pt/ZSM-5 Catalyst Precalcined at 790 K

	Pt–O		Pt–Pt							
	N	*R* (Å)	*N*	*R* (Å)	*N*	*R* (Å)	*N*	*R* (Å)	*N*[a]	*R* (Å)[a]
As received	6.3 ± 1.5	2.12 ± 0.03	4.2 ± 1.0	2.75 ± 0.01	—	—	4.5 ± 1	4.79 ± 0.02	4	5.42
Reduced at 620 K	1.8 ± 0.7	2.05 ± 0.03	10.3 ± 1	2.76 ± 0.01	3.9 ± 1	3.91 ± 0.02	6.4 ± 1	4.80 ± 0.02	8	5.43
Reduced at 790 K	1.5 ± 0.7	2.01 ± 0.03	10.1 ± 1	2.75 ± 0.01	4.5 ± 1	3.91 ± 0.02	7.6 ± 2	4.80 ± 0.02	7	5.42
Reduced at 790 K, then exposed to O_2 at 298 K	2.2 ± 0.7	1.98 ± 0.03	8.3 ± 1	2.74 ± 0.01	2.0 ± 1	3.92 ± 0.02	4.3	4.79 ± 0.02	5	5.41

[a] Values for this shell are complicated by multiple scattering; errors are thus difficult to assess.

TABLE 4

Activity of Pt/H–ZSM-5 Catalysts in Ethane Hydrogenolysis

	Calcined and reduced[a]		Reduced without calcination[a]	
	Turnover number at 673 K (s^{-1})	E_a[b] (kJ mol^{-1})	Turnover number at 673 K (s^{-1})	E_a[b] (kJ mol^{-1})
0.5% Pt	1.74 ± 0.1[c]	134 ± 7	0.014 ± 0.005	199 ± 10
1% Pt	1.58 ± 0.1[d]	133 ± 7	0.01 ± 0.005	188 ± 10

[a] Both reduction and calcination were carried out at 790 K.
[b] Measured in the range 573–723 K.
[c] Dispersion estimated from TEM data.
[d] Dispersion estimated from CO chemisorption studies.

the mean diameter of equivalent spherical particles is estimated from the bulk volume occupied by a platinum atom (1.51×10^{-29} m^3), and the results are given in Table 5. The sensitivity of the coordination number to particle size decreases as it approaches the bulk value of 12, causing the asymmetrical error bars quoted in parts of the table. EXAFS is at its most useful for particles <15 Å in diameter.

Previous studies have shown that calcination is important in stabilising small metal particles in ZSM-5 and other zeolites (*10, 16*). When the calcination step was omitted and a 0.5% Pt/ZSM-5 sample was reduced directly in hydrogen at 790 K, electron microscopy showed marked migration to the external surface and the growth of 120–150 Å particles. It is clear that the precise calcination temperature also makes a significant difference to the particle size. Calcination at 720 K rather than 790 K leads to smaller particles, even when both catalysts are subsequently reduced at 790 K. EXAFS shows the presence of metallic platinum after calcination at the higher temperature and we may speculate that particles produced during calcination act as nuclei for further growth during hydrogen treatment. The vibrational properties of the zeolite framework as a function of temperature may also have a role in determining ultimate particle size.

The larger particles found at the higher calcination temperature have a close-packed cubic structure and are not icosahedral. This can be seen from the nonnearest neighbour distances, which are found at $2^{1/2}a$, $3^{1/2}a$, and $2a$ (where a is the nearest neighbour distance), as required in cubic close packing. The nonnearest neighbour distances do not contribute significantly to the spectrum of the smaller particles, so their crystal structure cannot be deduced in this way. Moraweck and Renouprez (*3*) have attempted to demonstrate icosahedral particles in Y zeolite, by looking for splitting of the nearest neighbour peak into two components, with distances of $1.0a$ and ca $1.05a$. We do not believe that EXAFS is sufficiently sensitive to make this distinction without studying the variation of the spectrum with temperature. It is interesting to note that, despite many experimental studies in which theoretical considerations suggest that icosahedra might be expected (*17*), there is no reliable evidence for their existence as the majority species. Metal particles of fivefold symmetry have been observed in the electron microscope (*18*), and there is crystallographic evidence for the existence of icosahedra stabilised by ligands, such as phosphines (*19*), but there is still no reason to consider that the icosahedral structure is important in catalysis by metals. In a recent study of Rh/Al_2O_3 cata-

TABLE 5

Average Particle Size after Reduction at 793 K

	N_1	Average no. of atoms[a]	Average diameter[a] (Å)	
			EXAFS	Electron microscopy
0.5% loading, calcined at 720 K and reduced at 790 K	5.9 ± 1.3	13 ± 5	8.0 ± 0.7	—
0.5% Loading, calcined and reduced at 790 K	9.3 ± 1.0	120^{+75}_{+40}	15^{+4}_{-3}	13
1% Loading, calcined and reduced at 790 K	10.3 ± 1	220^{+175}_{-100}	18^{+5}_{-3}	16

[a] Derived as discussed in the text.

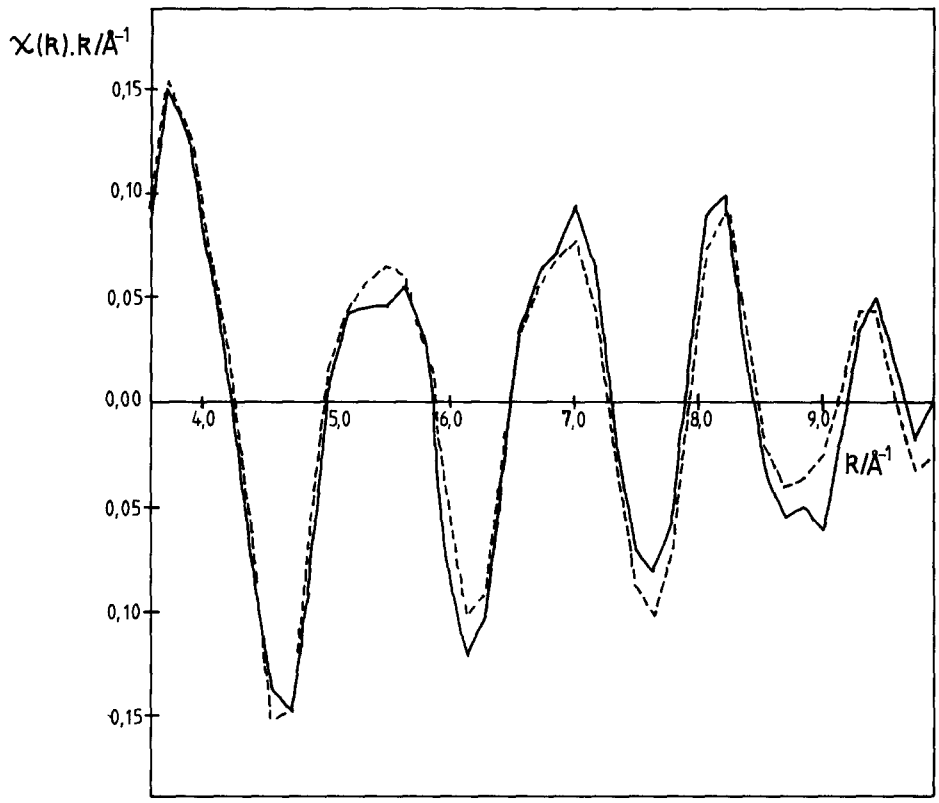

FIG. 2. Experimental (solid line) and calculated (dashed line) EXAFS for a 1% Pt/HZSM-5 catalyst which has been calcined and reduced at 790 K. Parameters used in the calculation are given in Table 3.

lysts it has been concluded that particles smaller than those reported here still have a cubic close-packed structure (*20*). That work used more intense synchrotron radiation than that available here, from a "wiggler" insertion source; better signal-to-noise ratios were therefore obtained.

Information on particle shape is less easy to obtain with certainty. As discussed by Greegor and Lytle (*15*), differently shaped particles posses different ratios of nonnearest to nearest neighbour CNs and can sometimes be distinguished. The relative values given in Tables 2 and 3 are consistent with spherical, cubic, or cylindrical particles, but not with rafts.

Knowing the average sizes of the particles allows us to speculate about their location. The ZSM-5 zeolite channels are 5–5.5 Å in diameter, so that the largest spherical particles which can be accommodated without lattice distortion will exist at channel intersections and have a diameter of about 7.5 Å. Thus it appears that metal particles resulting from the lower calcination temperature are of about the correct size to be located at channel intersections, while this is not the case where the calcination temperature is higher. We cannot rule out the possibility that larger metal particles may be accommodated by distortion of the zeolite framework, since this has been observed in Pt/Na–Zeolite X (*16*), or that the larger particles are cylindrical in shape. If all the particles were cylindrical and accommodated in the wider zeolite channels the average length would be ca. 30 Å. This seems improbable, since the catalytic turnover num-

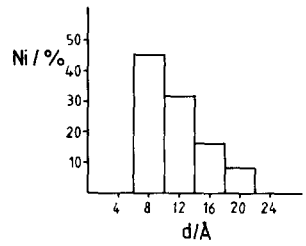

FIG. 3. Particle size histogram obtained by electron microscopy for the 0.5% Pt/HZSM-5 catalyst after reduction at 790 K. Note that the electron microscope is unable to detect particles of diameter < ca. 6 Å.

bers observed are high, suggesting that most of the particle surface is accessible. It seems more likely that the observed average reflects the coexistence of cylindrical particles in the channels, spherical particles at channel intersections, larger particles formed by distorting the zeolite framework, and some metal at the external surface. Electron microscopy indicates, however, that only a small fraction of the metal is at the external zeolite surface. An additional possibility is that the metal particles can distort or encapsulate part of the zeolite framework, as suggested by Gallezot (*34*). This could explain why the Pt–O coordination numbers increase in the larger particles.

It is of interest to compare the average particle size deduced from EXAFS with the histogram distribution generated from electron microscopy measurements, and shown in Fig. 3. The average nearest neighbour coordination number has been obtained from the histogram by inverting the procedure used to obtain the particle sizes given in Table 5, for each part of the histogram. The overall average is then obtained from

$$N_{av} = \sum (F_i \cdot n_i \cdot N_i) / \sum (F_i \cdot n_i),$$

where F_i is the fraction of particles in the ith part of the histogram, n is the number of atoms in a particle of this size, and N_i is the relevant nearest neighbour coordination number. We conclude that the average particle measured by electron microscopy is 12.75 Å in diameter, contains 72 atoms, and has a mean nearest neighbour coordination number of 9.3. The agreement with the values derived from EXAFS is very encouraging.

The contraction of interatomic distances in small particles has now been observed so often that it should be regarded as a general feature. Almost all EXAFS studies of sufficiently small clusters have reported contractions, and metals studied include platinum, nickel, rhodium, and gold (*3, 4, 20, 21*). Only in the case of palladium evaporated onto mica and studied by electron microscopy has it been suggested that the nearest neighbour distance is unchanged with respect to the bulk (*22*).

The largest contraction observed here is 3.6%, for particles containing an average of 18 atoms. This is at the top range reported for clusters and suggests that there may be some influence of interaction with the zeolite framework.

2. *Platinum–Oxygen Bonding*

An interesting feature of the EXAFS results is the observation of platinum–oxygen distances in the range 1.9–2.05 Å, in each of the reduced catalysts studied. There appears to be a distinction between Pt–O bonding in the larger particles, where the distance is close to 2.0 Å and the Debye–Waller factor is large (0.02 Å^2), and the smaller particles indicated in Table 1, where the distance is significantly shorter and the Debye–Waller factor is quite low, 0.008 Å^2.

We do not believe that this metal–oxygen bonding is the result of incomplete reduction of an oxide precursor. All of the catalysts have been exposed to flowing hydrogen at 790 K, well above the temperature normally required to reduce oxidised platinum particles of this size (ca. 400 K (*23*)). It seems much more probable that the Pt–O distances result from coordination of platinum in small particles to the framework oxygen of the zeolite and we note that similar M–O distances have been reported for Pt/Al_2O_3 catalysts by Lagarde *et al.* (*24*), and ascribed to metal-support interactions. Not surpris-

ingly, the interaction between metal and framework oxygen appears to be much stronger for the small particles, in the zeolite calcined at 720 K, than it is for the larger particles, in the zeolites calcined at the higher temperature. We have searched for but found no evidence of long metal–oxygen bonds (ca. 2.7 Å) of the type reported by van Zon *et al.* (*25*).

We can rule out the possibility of individual platinum ions coordinated to the zeolite framework, of the sort that can be stabilised in the faujasites and in zeolite A (*26*). There is only one relevant crystallographic study, which examines nickel exchanged into ZSM-5 (*5*). Two coordination sites were located, one at a position near the centre of a six-membered ring, where the larger Pt^{2+} ion could not penetrate, and the second in a channel. This nickel ion was three-coordinate, but with Ni–O bonds much longer, at ca. 3 Å, than observed here. Also, if isolated Pt^{2+} ions were important, we would expect to see a greater contribution in the zeolite with the lower calcination temperature, and consequently a higher Pt–O coordination number. Instead, this coordination number appears to increase with particle size, supporting the suggestion that most of the particles are inside the zeolite framework.

It is significant that distinctly different Pt–O distances are observed for the different sizes of metal particle. For the smallest particles, the distance is ca. 1.92 Å, rising for the larger particles to ca. 2.03 Å. This suggests that the particles are located at different places in the zeolite structure, with the smaller particles perhaps in the channels, and the larger at the channel intersections as discussed above.

3. Relationship to Catalytic Reactivity

Catalytic measurements reported here and elsewhere indicate that these Pt/ZSM-5 catalysts have high turnover numbers for a range of reactions, including hydrogenolysis, alkane isomerisation, and alkane aromatization. The results in Table 3 show that the specific activity for hydrogenolysis is ca. 2 orders of magnitude higher when the platinum particles are relatively small and located within the zeolite framework than when they are large and at the external surface. Similar results have been reported previously for aromatization (*1*). Factors which may play a part in generating the increased activity of the zeolite encapsulated catalyst include particle size, electronic structure, and metal–zeolite synergy. Hydrogenolysis is the best recognised structure sensitive reaction, and for a number of metals, including nickel, platinum, and osmium, the specific rate goes through a maximum at about the particle size studied here (*27–29*). In the case of platinum, the narrower *d* band and greater free atom character of the small cluster may favour stronger ethane adsorption, and therefore higher hydrogenolysis activity for small particles. The role of size and electronic structure for nickel and osmium is much less clear, since both metals are at the top of the "volcano plots" for their respective rows of the Periodic Table (*27*). It would be of interest to see a study of the structure sensitivity of a metal such as iron or rhenium, which sits on the strong adsorption side of the volcano maximum.

Any explanation involving a dual-function type of synergy can be ruled out, since the ZSM-5 framework has no activity in ethane hydrogenolysis in the absence of a metal. At higher temperatures, however, the dehydrogenation activity associated with the zeolite acid sites may have to be considered. Dual functionality, however, seems to be the major factor in explaining the metal–zeolite synergy reported earlier for the aromatization of lower alkanes (*1*).

The existence of an electronic interaction between the metal particles and the zeolite framework is more contentious. It has been forcibly argued elsewhere, on the basis of large metal-core level shifts observed in X-ray photoelectron spectra, that metal particles in the ZSM-5 matrix are electron deficient (*2*). Although it is difficult to differenti-

ate initial and final state effects for small particles (*30*), the metal–zeolite case represents the most likely situation where electronic interaction between a metal and its host can be expected, since the zeolite surrounds the metal particle. It has been demonstrated elsewhere that electronic interaction between a metal and a support has a range of <5 Å (*31*). Within a zeolite, however, all of the surface atoms in the metal particles will be very close to the framework, and may be subject to electronic modification. Additional experimental studies are required to determine the fraction of the observed XPS shift which is attributable to final state effects. The comparative intensity of the white line at the X-ray absorption edge has also been interpreted as indicating metal-support electron transfer. Recently van Santen *et al.* (*33*), have suggested that changes in white line intensities may also have their origin in final state effects.

Last, a brief word must be said about the reactivity of the reduced metal particles to oxygen. The relatively extensive oxidation indicated in Tables 1 and 3 is not unexpected for small platinum particles; indeed, slow complete oxidation occurs for the somewhat larger (mean diameter 16 Å) particles formed in the Pt/SiO_2 reference catalyst EUROPT 1 (*23, 32*). The reactivity to oxygen again shows that the platinum particles are accessible to the gas phase and thus available for catalytic reaction.

CONCLUSIONS

Platinum catalysts have been prepared by a combination of impregnation and exchange into the zeolite ZSM-5. After calcination, platinum particles with diameter in the range 8–18 Å were obtained, the size depending on the calcination temperature. Evidence has been found for Pt–oxygen bonding, with a bond length of 1.9–2 Å, and this bonding is attributed to attachment to the zeolite framework. The catalysts have higher specific activity for ethane hydrogenolysis than materials where the platinum is in large particles at the exterior of the zeolite and reasons for this are discussed.

ACKNOWLEDGMENTS

We are grateful to BP Research (Sunbury-on-Thames) for the use of their *in situ* cell, to Mrs. G. J. Tuleuova (Zelinsky Institute of Organic Chemistry, Moscow) for performing the catalytic measurements, and to Dr. V. A. Zaikovski (Institute of Catalysis, Novosibirsk) for carrying out the electron microscopy. We thank the UK Science and Engineering Research Council (SERC) for their support of this work, in particular through a Senior Visiting Fellowship to ESS and a fellowship to PDAP. The helpful comments of a referee are also acknowledged.

REFERENCES

1. Bragin, O. V., Shpiro, E. S., Preobrazhensky, A. V., Isaev, S. A., Vasina, T. V., Dyusebina, B. B., Antoshin, G. V., and Minachev, Kh. M., *Appl. Catal.* **27,** 219 (1986).
2. Antoshin, G. V., Shpiro, E. S., Tkachenko, O. P., Nikishenko, S. B., Avaev, V. I., Ryashenzeva, M. A., and Minachev, Kh. M., *in* "Proc. 7th Intern. Congr. Catalysis, Tokyo, 1980," p. 302. Kodansha/Elsevier, Tokyo/Amsterdam, 1981.
3. Moraweck, B., and Renouprez, A. J., *Surf. Sci.* **108,** 35 (1981).
4. Gallezot, P., Weber, R., Della Betta, R. A., and Boudart, M., *Z. Naturforsch. A* **34,** 40 (1979); Gallezot, P., and Bergeret, G., *J. Catal.* **72,** 294 (1981); Gallezot, P., *in* "Homogeneous and Heterogeneous Catalysis" (Yu. Yermakov and V. Likholobov, Eds.). VNU Science Press, Ulrich, 1983.
5. Wangjin, Z., Qin, Y., Guanglie, L., Wangrong, L., Shuju, W., Youshi, Z., and Bingxsong, L., *in* "New Developments in Zeolite Science and Technology" (Y. Murakami, A. Iijima and J. W. Ward, Eds.), p. 415. Kodansha Elsevier, Tokyo/Amsterdam, 1986.
6. Koningsberger, D. C., and Prins, R., Eds., "X-Ray Absorption," Chap. 8. Wiley, New York, 1988.
7. M. J. Phillips and M. Ternan, Eds., "Proc. 9th Intern. Congr. Catal., Calgary, 1988, Vol. 5." Chemical Inst. Canada, Ottawa, 1988.
8. Joyner, R. W., Martin, K. J., and Meehan, P., *J. Phys. C* **20,** 4005 (1987).
9. Joyner, R. W., and Meehan, P., *Vacuum* **33,** 691 (1983).
10. Shprio, E. S., Tuleuova, G. J., Zaikovskii, V. A., Tkachenko, O. P., Vasina, T. A., Bragin, O. V., and Minachev, Kh. M., *in* "Zeolites as Catalysts, Sorbents and Detergent Builders" (H. G. Karg and J. Weitkamp, Eds.), p. 145. Elsevier, Amsterdam, 1989.
11. Lee, P. A., and Pendry, J. B., *Phys Rev. B* **11,** 2795 (1975).

12. Gurman, S. J., Binstead, N., and Ross, I., *J. Phys. C:* **17,** 143 (1984).
13. Pantos, E., and Firth, D., *in* "EXAFS and Near Edge Structure," (A. Bianconi, L. Incoccia, and S. Stipcich, Eds.). Springer-Verlag, Berlin, 1983.
14. Joyner, R. W., *in* "Characterisation of Catalysts" (J. M. Thomas and R. M. Lambert, Eds.). Wiley, Chichester, 1980.
15. Greegor, R. B., and Lytle, F. W., *J. Catal.* **63,** 476 (1980).
16. Jaeger, N. I., Rathousky, J., Schulz-Ekloff, G., Svennson, A., and Zukal, A., *in* "Zeolites, Facts, Figures, Future" (P. A. Jacobs and R. A. van Santen, Eds.), p. 1005. Elsevier, Amsterdam, 1989.
17. Burton, J. J., *Catal. Rev.* **9,** 209 (1974); Gordon, M. B., Cyrot-Lackmann, F., and Desjonqueres, M. C., *Surf. Sci.* **68,** 359 (1979); **80,** 159 (1979); Solliard, C., *Surf. Sci.* **106,** 58 (1981); Khanna, S. N., Bucher, J. P., Buttet, J., and Cyrot-Lackmann, F., *Surf. Sci.* **127,** 165 (1983).
18. Yacaman, M. J., Fuentes, S., and Dominiques, J. M., *Surf. Sci.* **106,** 472 (1981).
19. Briant, C. E., Theobald, B. R. C., White, J. W., Bell, L. K., Mingos, D. M. P., and Welch, A. J., *J. Chem. Soc., Chem. Commun.,* 201 (1981).
20. Johnston, P., Joyner, R. W., and Pudney, P. D. A., *J. Phys.: Condensed Matter* **1,** SB171 (1989).
21. Copper and nickel: Apai, G., Hamilton, J. F., Stohr, J., and Thompson, A., *Phys. Rev. Lett.* **43,** 165 (1979); iron and chromium: Montano, P. A., Purdum, H., Shenoy, G. K., Morrison, T. I., and Schulze, W., *Surf. Sci.* **156,** 228 (1985); gold: Balerna, A., Bernieri, E., Picozzi, P., Reale, A., Santucci, S., Burattini, E., and Mobilio, S., *Phys. Rev. B* **31,** 5058 (1985); platinum: see Refs. (*3*) and (*4*).
22. Heinemann, K., and Poppa, H., *Surf. Sci.* **156,** 265 (1985).
23. Bond, G. C., and Gelsthorpe, M. R., *Appl. Catal.* **35,** 169 (1987).
24. Lagarde, P., Murata, T., Vlaic, G., Freund, E., Dexpert, H., and Bournonville, J. P., *J. Catal.* **84,** 333 (1983).
25. van Zon, J. B. A. D., Koningsberger, D. C., van't Blik, H. F. T., Prins, R., and Sayers, D. E., *J. Chem. Phys.* **80,** 3914 (1984); **82,** 5742 (1985).
26. Kellerman, R., and Klier, K., *in* "Surface and Defect Properties of Solids" (J. M. Thomas and M. W. Roberts, Eds.), Vol. 4, p. 1. Chem. Soc., London, 1975.
27. Sinfelt, J. H., *Catal. Rev.* **3,** 175 (1970).
28. Guczi, L., and Gudkov, B. S., *Kinet. Catal. Lett.* **9,** 343 (1978).
29. Jackson, S. D., Moyes, R. B., Wells, P. B., and Whyman, R., *J. Catal.* **86,** 342 (1984).
30. Wertheim, G. K., DiCenzo, S. B., and Youngquist, S. E., *Phys. Rev. Lett.* **51,** 2310 (1983).
31. Joyner, R. W., Pendry, J. B., Saldin, D. K., and Tennison, S. R., *Surf. Sci.* **138,** 84 (1984).
32. Joyner, R. W., *J. Chem. Soc. Faraday Trans. 1* **76,** 357 (1980).
33. van Santen, R. A., *et al.,* Personal communication, to be published.
34. Gallezot, P., *Catal. Rev. Sci. Eng.* **20,** 121 (1979).